Lab on a stick: multi-analyte cellular assays in a microfluidic dipstick

Article

Accepted Version

For table of contents:

Lab on a Stick: Multi-Analyte Cellular Assays in a Microfluidic Dipstick

Nuno M. Reis*[a], Jeremy Pivetal[b], Ana L. Loo-Zazueta [a], João M.S. Barros[b], and Alexander D. Edwards*[b]

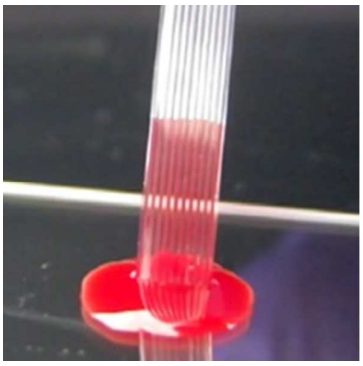

A Lab-on-a-Stick concept for simple, rapid, multiplexed and quantitative cellular bioassays in a dipstick format with the benefits of microfluidics.

Journal Name

ARTICLE

Lab on a Stick: Multi-Analyte Cellular Assays in a Microfluidic Dipstick

Received 00th January 20xx,
Accepted 00th January 20xx

DOI: 10.1039/x0xx00000x

www.rsc.org/

Nuno M. Reis*[a], Jeremy Pivetal[b], Ana L. Loo-Zazueta [a], João M.S. Barros[b], and Alexander D. Edwards*[b]

A new microfluidic concept for multi-analyte testing in a dipstick format is presented, termed "Lab-on-a-Stick", that combines the simplicity of dipstick tests with the high performance of microfluidic devices. Lab-on-a-Stick tests are ideally suited to analysis of particulate samples such as mammalian or bacterial cells, and capable of performing multiple different parallel microfluidic assays when dipped into a single sample with results recorded optically. The utility of this new diagnostics format was demonstrated by performing three types of multiplex cellular assays that are challenging to perform in conventional dipsticks: 1) instantaneous ABO blood typing; 2) microbial identification; and 3) antibiotic minimum inhibitory (MIC) concentration measurement. A pressure balance model closely predicted the superficial flow velocities in individual capillaries, that were overestimated by up to one order of magnitude by the Lucas-Washburn equation conventionally used for wicking in cylindrical pores. Lab-on-a-stick provides a cost-effective, simple, portable and flexible multiplex platform for a range of assays, and will deliver a new generation of advanced yet affordable point-of-care tests for global diagnostics.

Introduction

The benefits of bioassay miniaturization are well described[1] and in recent years increased interest in decentralised diagnostics has catalyzed the rapid development of several generations of microfluidic Lab-on-a-chip systems including Lab-in-a-foil,[2] Lab-on-paper,[3] Patterned paper,[4–6] Lab-on-a-disk,[7] Lab-on-a-DVD,[8] Lab-on-a-syringe[9] and 'Shrinky-dink' microfluidics.[10] Dipsticks are a far older testing format familiar in environments as diverse as the garden (soil pH strips), bathroom (urinalysis strips and home pregnancy lateral flow tests, or pharmacy (blood glucose or urinalysis strips), and can analyze targets ranging from protons (pH paper) through to proteins.[11] Although dipstick tests are low cost and simple to use, they are unable to assay particulate samples such as cellular assays that measure or detect live cells.[12] Current Lab-on-a-chip systems are unable to compete directly with lateral flow tests with respect to simplicity of use and manufacturing costs. There remains a need for a miniaturised platform capable of combining the reduced sample volume and assay times of microfluidic systems together with the simplicity and low cost of dipstick tests for cellular analysis.

New approaches for one-step microfluidic bioassays have been recently reported, mainly fabricated from PDMS. Samples are traditionally loaded in microfluidic devices using syringes,[13] electrokinetics,[14] or centrifugal forces,[7] however pressure-driven delivery methods have the disadvantage of requiring external bulking equipment. Inspired by lateral flow tests new miniaturised devices were recently developed operating by capillary action.[15–17] The advantages and applications of microfluidic diagnostic devices working with capillary action is extensively discussed elsewhere.[18–20] In-situ delivery of assay reagents in capillary-driven microfluidic devices is not trivial, and new approaches included inkjet printing;[15] embedding in a substrate-copolymerized hydrogel network;[21] use of a dissolvable reagents membrane;[22] or trapping within a soluble PEG-based coating.[23]

Fluorinated ethylene propylene (commercially known as Telfon® FEP) is a copolymer of hexafluoropropylene and tetrafluoroethylene, belonging to a class of fluorocarbon-based polymers with multiple strong carbon–fluorine bonds characterised by a refractive index close to that of water and hydrophobic surface. Our research group has recently pioneered rapid and high sensitivity sandwich immunoassays in FEP microfluidic devices[24–26] characterised by simple connectivity, easy to multiplexing and low manufacturing cost. The optical properties of FEP favours optical interrogation of bioassays with e.g. smartphones,[26] however the hydrophobic nature of Teflon® FEP however remains incompatible with the capillary action required for simple, one-step microfluidic immunoassays.

We present in Fig. 1 a new microfluidic Lab-on-a-Stick ap-

[a] Department of Chemical Engineering, Loughborough University, Leicestershire, LE11 3TU, UK. E-mail: n.m.reis@lboro.ac.uk; Fax: +44(0) 1509 223 923; Tel. +44(0) 1509 222 505
[b] Reading School of Pharmacy, University of Reading, Whiteknights, Reading RG6 6AD, UK.E-mail: a.d.edwards@reading.ac.uk; Fax: +44 (0) 118 378 6562; Tel: +44(0) 118 378 4253

† Electronic Supplementary Information (ESI) available: film showing blood aspiration by capillary action in the hydrophilic coated MCF; film showing blood agglutination in microcapillaries; ESI document including supplementary methods and supplementary results. See DOI: 10.1039/x0xx00000x

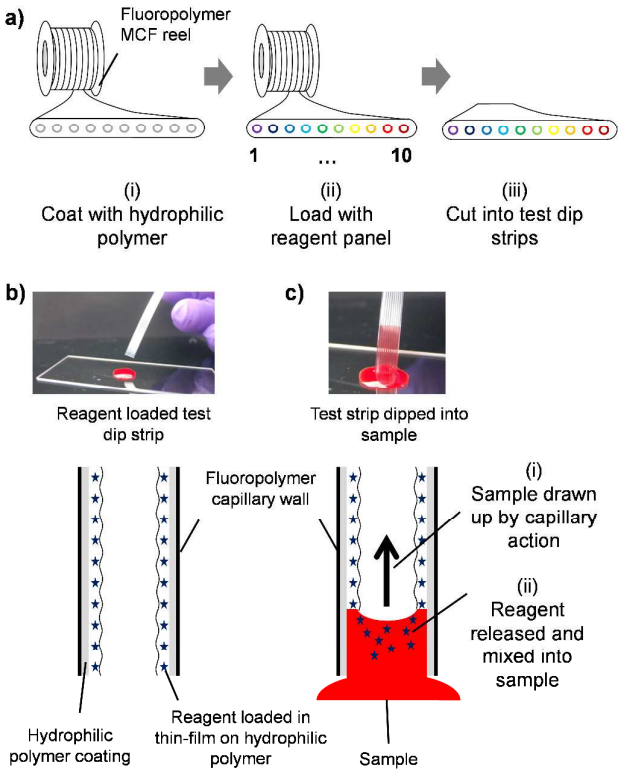

Fig. 1 Lab-on-a-Stick assay concept. a) Mass manufacturing of multiplex test strips requires three simple steps: i) the internal surface of melt-extruded fluoropolymer MCF containing 10 microcapillaries is bulk coated with a hydrophilic crosslinked PVOH layer. ii) Individual capillaries are loaded in bulk with reagent solutions, and then excess reagents removed leaving a thin film of reagent deposited on the inner surface of the microcapillaries which is then dried. iii) Single dip-strip test devices are prepared by trimming the long MCF reel. b) Each microcapillary within the dip-strip contains a hydrophilic coating covered with a thin film of dried reagent(s). c) When dipped into an aqueous fluid such as blood, i) the sample is drawn up by capillary action into all 10 microcapillaries and ii) reagents quickly released, performing multiple microfluidic assays.

proach which uniquely combines key features of dipstick tests with the fluidic format and capabilities of microfluidic Lab-on-a-Chip systems, namely: 1) simple use – just dip and read; 2) low cost scalable manufacture; 3) reagents stored dry and released into the sample; and 4) reagents in different locations allowing multiple tests to be performed on a single sample. Since Lab-on-a-Stick is a microfluidic system, it is suitable for particulate samples including cellular analysis.[27,28] Lab-on-a-Stick test strips are produced by surface modification of fluoropolymer microcapillary film (MCF), a low-cost mass manufactured microengineered material capable of performing multiple quantitative and sensitive assays in an array of microfluidic channels embedded in an optically transparent ribbon.[29] The excellent optical transparency of the fluoropolymer MCF material is ideal for naked eye detection or measurement with portable, inexpensive optoelectronic equipment including a smartphone camera[26] that cannot be matched by a bundle of individual microcapillaries as previously explained in Edwards et al.[30] In contrast to previous work that demonstrated biomarker measurement in heterogeneous immunoassays in fluoropolymer MCFs, the novelty of the Lab-on-a-Stick lies in the instant homogeneous assay format and the application to a broad range of different assays for testing cellular samples.

Experimental

Hydrophilic coating of microcapillary film. MCF was produced by Lamina Dielectrics Ltd (Billingshurst, West Sussex, UK) from Teflon® FEP (Dupont, USA) using a melt-extrusion process,[29] and consisted of an array of 10 parallel microcapillaries with a mean hydraulic diameter of 206 ± 12.6µm. The fluoropolymer MCF was subsequently modified by coating the inner surface of the microcapillaries with a permanent hydrophilic layer of PVOH. This involved recirculating at a flow rate of 50 mL/h overnight a volume of 100 mL of a 5 mg/mL solution of PVOH in water (MW 13,000-23,000, >98% hydrolysed for ABO blood grouping experiments; MW 146,000-186,000, >99% hydrolysed for bacteria and MIC testing – all from Sigma-Aldrich, UK). A 6 m long fluoropolymer MCF was attached to a FPLC P-500 Pharmacia Biotech pump using Upchurch flangeless tube fittings (Kinesis, UK). The PVOH coating was then crosslinked with glutaraldehyde by manually filling the MCF with a freshly prepared 5 mg/mL of PVOH solution containing 5 mM of glutaraldehyde (Sigma-Aldrich, UK) and 5 mM HCl (Sigma-Aldrich, UK) for 2 hours at 37°C, followed by manual washing with water and drying with multiple changes of air using a 50 mL syringe.

Measurement of contact angle. The equilibrium contact angle for both uncoated and PVOH coated FEP microcapillary film was determined using the capillary rise method. A 15 cm long dried MCF strip was immersed in deionised water in a transparent reservoir, and the difference between liquid level within each capillary and liquid level in the reservoir, H recorded. For uncoated MCF (hydrophobic, yielding negative liquid rise) the strip was immersed until a meniscus was visible within all 10 capillaries. For hydrophilic (positive liquid rise) the strip was immersed 10 mm into the water and meniscus allowed to equilibrate before recording the position. Due to the nature of melt-extrusion process, capillaries at the edge are slightly flattened and smaller because of the drawing ratio, consequently the equilibrium contact angle in the elliptical microcapillaries was estimated from liquid height based on a modified Young-Laplace's equation:

$$H = \frac{\gamma \cos\theta}{\rho g}\left(\frac{1}{a}+\frac{1}{b}\right) \qquad (1)$$

where γ is surface tension for water (taken as 72.8 mN/m), ϑ is the contact angle (in radians), ρ is the density of water (taken as 997.1 kg/m^3), g is the gravitational acceleration, and a and b the width and depth, respectively, in meters of the elliptical capillary as measured by analysing several cross-sections of the MCF using optical microscopy and Image J (NIH, USA).

Reagent loading. The method used for loading reagents is simple, scalable and rapid (Fig. 1a and Fig. 2). Concentrated solutions of assay reagent or reagent mixtures were filled into

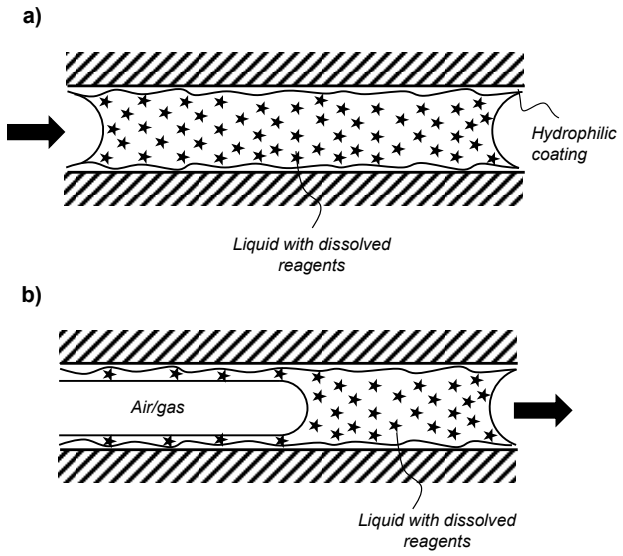

Fig. 2 Reagents loading in the PVOH-coated microcapillaries. a) Capillaries are fully loaded with reagents solution. b) Excess liquid is removed by aspirating air or inert gas, leaving behind a thin film of reagents deposited on the wall of the capillaries.

individual capillaries (Fig. 2a) in bulk reels of 0.5-5.0 meters of polymer coated MCF. After a short incubation (from 5 minutes up to 2 hours), the bulk loading solution was removed leaving behind a thin yet uniform liquid film containing reagents (Fig. 2b), and if required, the deposited liquid reagent film was gently dried with dry air or nitrogen.

Efficiency of reagent loading. For quantitation of reagents deposition in the PVOH coated MCF, individual microcapillaries within a reel of 20-2,000 mm were filled using a 30G needle with the appropriate reagent solutions, and after 5 min the excess loading solution was removed by manually injecting air into all capillaries with a 50 mL plastic syringe. The released reagent concentrations were measured by dipping one or more 80 mm long loaded MCF strip into water and allowing microcapillaries to fill completely by capillary action, incubating for 5 min, and then completely removing released solution, followed by quantitation of released reagent concentration in eluted sample by UV absorbance (antibody), enzymatic end-point assay (glucose), or by quantitative LC-MS (antibiotics).

Proof-of-concept Lab-on-a-Stick assays. For ABO blood typing, microcapillaries were loaded with ALBAclone® Monoclonal ABO antisera anti-A, anti-B or anti-D reagents used as supplied, and devices tested with simulated whole blood ALBAcheck®-BGS (Alphalabs, UK), and strips recorded with a CCD camera. For bacterial identification by fermentation, one colony of *E. coli* (ATCC 25922), *S.* typhimurium (strain SL3261) or *P. aeruginosa* (ATCC 27853) on LB agar plates was re-suspended in 100 µl of fermentation broth (0.1g/L Trypticase, 5g/L NaCl) containing 1 mg/mL of phenol red (all sourced from Sigma-Aldrich, UK). Test strips loaded with the indicated panel of sugars were then dipped into each bacterial suspension and incubated for 4h at 37°C. For antibiotic resistance measurement, a 30 cm long PVOH coated MCF were loaded with a 2-fold serial dilution of the indicated antibiotic at concentrations ranging from 100 to 0 µg/ml. The MCF was then trimmed into 40 mm long test strips and dipped into samples containing one bacterial colony re-suspended in 100 µl of Muller Hinton media and diluted 10,000 fold in the same media supplemented with 1 mg/mL of resazurin and incubated overnight at 37°C. Colorimetric microbiology test strips were imaged with a Fujifilm XF1 or Canon S120 camera using white background illumination.

Results and discussion

A core step in the development of this novel Lab-on-a-Stick concept devices is the modification of the internal surface of a 10-bore ~200 µm internal diameter MCF manufactured from Telfon-FEP® (Fig. 3a) - previously used in our research group to perform rapid, high sensitivity ELISA[25,30] - with a hydrophilic coating consisting of cross-linked PVOH which introduced two new features with a single modification step. Firstly, the PVOH coating dramatically reduced the contact angle of the FEP microcapillaries allowing sample uptake by capillary action. Secondly, the PVOH coating also facilitated simple deposition of a very thin film of reagents within the capillaries for in-situ reagent delivery. These two key steps were studied in detail.

Although commercially known as a non-stick surfaces, fluoropolymers like FEP have been previously coated with cross-linked low-molecular weight PVOH[31] or high-molecular weight PVOH,[32] the last is extensively described also in US Patent 7,179,506 B2. Consequently, this work has fully focused on surface modification of FEP microcapillaries with PVOH, to our knowledge something that remained unreported up to date.

Liquid rise in FEP-Teflon microcapillaries

The equilibrium contact angle measured with liquid rise experiments and Young-Laplace equation for uncoated fluoropolymer MCF was very high, with a mean value of 123 ± 1.6 degrees across the whole MCF strip (Fig. 3b). The dimensions of individual microcapillaries are shown in Table 1. Capillaries were fitted to an ellipse, where *a* represents the major axis (capillary width) and *b* the minor axis (capillary depth). The high contact angle of uncoated microcapillaries is linked to the very hydrophobic nature of FEP-Teflon material. The coating procedure reduced the contact angle to 67 ± 2.2 degrees (Fig. 3b), making it possible to drawn up aqueous samples such as whole blood by capillary action without the need of hydraulics. Liquid rise in the parallel array of PVOH coated microcapillaries was found to be fast yet very consistent across the whole 10-bore strip. This is further demonstrated by the film provided in Electronic Supplementary Information showing drawn up of whole human blood. When capillaries were dried by manually blowing air through the strips using a 50 mL plastic syringe, and liquid height measurements repeated two further times, we noted that the gluteraldehyde crosslinking was important to obtain a stable coating with a contact angle that did not change during reagent loading and sample testing. A detailed

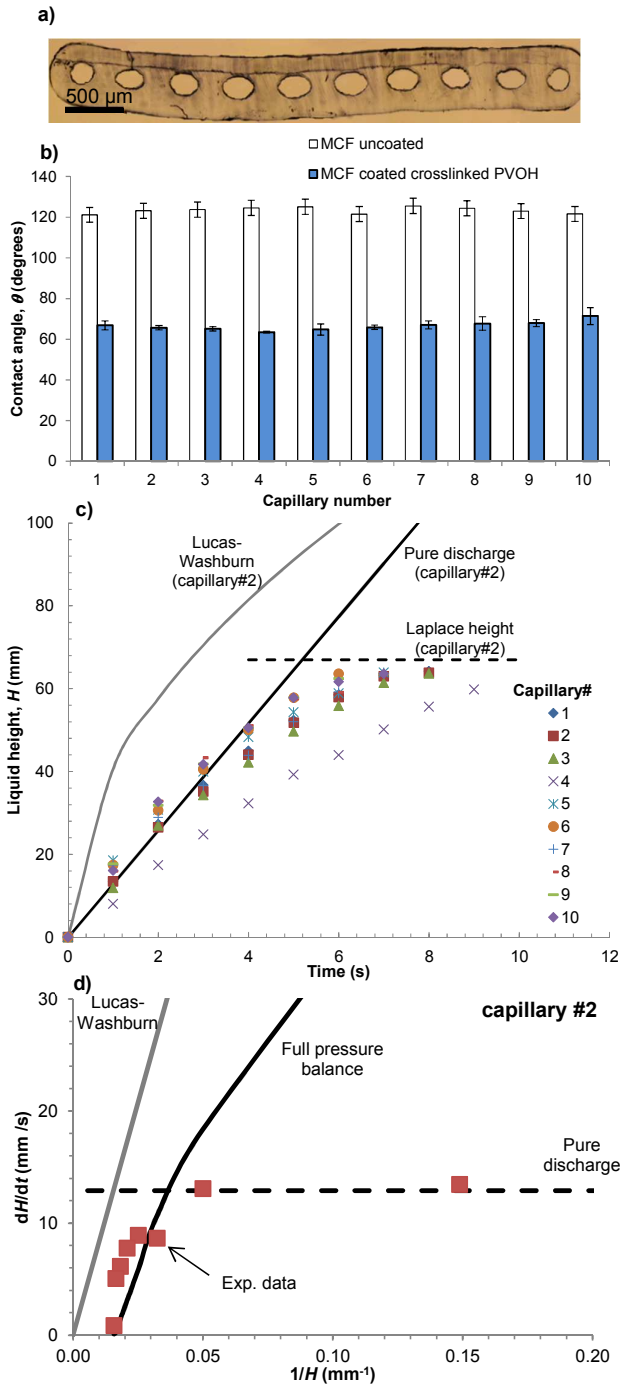

Fig. 3 Capillary flow in vertical FEP microcapillaries. a) Microphotograph showing the cross section of the 10-bore FEP microcapillary film. b) Equilibrium contact angle in individual microcapillaries for the MCF uncoated and MCF coated with crosslinked PVOH; error bars represent one standard deviation from at least three experimental replicas. c) Water rise in individual microcapillaries, showing the initial liquid rise follows a pure discharge system that cannot be modelled by Lucas-Washburn equation. d) Modelling of superficial flow velocity, d*H*/d*t* in random capillary number 2.

characterisation of the inner surface of multiple PVOH-coated microcapilaries by SEM and AFM revealed the PVOH-coating was homogeneous along and across the microcapillaries (see Supplementary Methods and Figs. S4 and S5 in ESI), an important feature for obtaining consistent liquid rise results. The time required for the liquid to reach the maximum (equilibrium) liquid height set by the Laplace pressure was in the order of 10 seconds (Fig. 3c).

Liquid rise in the hydrophilic microcapillaries was successfully modelled by performing a full pressure balance to the microcapillaries:

$$\Delta P_L = \Delta P_H + \Delta P_F \quad (2)$$

The Laplace pressure drop across the air-water-wall interface is given by:

$$\Delta P_L = \frac{4\gamma}{d_h}\cos\theta \quad (3)$$

and the pressure head in the liquid height *H* given by:

$$\Delta P_H = g\rho H \quad (4)$$

The pressure drop imposed by frictional losses in the capillary is given by the Darcy-Weisbach equation:

$$\Delta P_F = f_D \frac{\rho u^2}{2d_h} H \quad (5)$$

For laminar flow regime, the Darcy friction factor f_D is given by:

$$f_D = \frac{64}{\mathrm{Re}} \quad (6)$$

where the Reynolds number, *Re* is given by:

$$\mathrm{Re} = \frac{\rho u d_h}{\mu} \quad (7)$$

The Laplace pressure in elliptical capillaries is more accurately represented by Young-Laplace's law shown in Equation (1), however for simplicity of the model capillaries were approximated in Equation (3) by considering the hydraulic diameter, d_h:

Table 1. Size of individual microcapillaries in Telfon FEP MCF and maximum (equilibrium) liquid height, *H* in PVOH coated MCF

Capillary#	Major axis capillary, *a* (µm)	Minor axis capillary, *b* (µm)	Hydraulic diameter, d_h (µm)	Maximum, equilibrium height, *H* (mm)
1	190.7	207.1	198.4	58.9 ± 3.73
2	182.7	249.5	208.5	58.0 ± 1.73
3	200.4	245.1	219.4	56.7 ± 1.63
4	202.6	271.9	229.7	57.2 ± 0.59
5	200.0	282.4	230.8	54.1 ± 3.90
6	201.6	283.3	232.3	51.7 ± 1.51
7	205.6	272.1	232.0	49.5 ± 2.77
8	196.1	238.9	214.4	52.3 ± 5.16
9	182.7	250.9	208.9	52.8 ± 2.80
10	192.0	200.4	196.1	48.3 ± 7.44

$$d_h = \frac{4A}{P} \quad (8)$$

where A is the cross-section area of the capillary, and P the perimeter.

For horizontal flow in hydrophilic microcapillaries the pressure head term ΔP_H in Equation (2) can be neglected, and the pressure balance solved in respect to the superficial flow liquid velocity, $u(t)$ or dH/dt:

$$u(t) \equiv \frac{\mathrm{d}H}{\mathrm{d}t} = \frac{d_h}{32\mu} 4\gamma \cos\theta \frac{1}{H} \quad (9)$$

Integration of Equation (9) leads to the well-known Lucas-Washburn equation that governs capillary action in cylindrical pores, including paper[33] and nitrocellulose test strips:

$$H(t) = \left[\frac{1}{4\mu} \gamma \cos\theta \, d_h \, t \right]^{1/2} \quad (10)$$

For capillary flow in vertical hydrophilic microcapillaries the full pressure balance in Equation (2) yields the following analytical solution for dH/dt:

$$\frac{\mathrm{d}H}{\mathrm{d}t} = \frac{d_h}{32\mu} \left[4\gamma \cos\theta \frac{1}{H} - \rho g d_h \right] \quad (11)$$

Surprisingly, it was observed that liquid height, H increased linearly with time (Fig. 3c), suggesting capillary flow in the microcapillaries at the initial stages of capillary rise (i.e. up to 40% of Laplace height) is not governed by surface tension, and rather dH/dt followed the superficial flow velocity predicted for gravity discharge from a vertical capillary (Fig. 3d). The pressure balance for gravity emptying of a capillary can be written as:

$$\Delta P_H = \Delta P_F \quad (12)$$

Note the pressure balance in Equation (12) requires the flow resistance force to have opposite direction to that of the head pressure. The pressure balance can be solved yielding:

$$\frac{\mathrm{d}H}{\mathrm{d}t} = \frac{\rho g \, {d_h}^2}{32\mu} \quad (13)$$

Equation (13) can be integrated in respect to time yielding:

$$H(t) = \frac{\rho g \, {d_h}^2}{32\mu} t \quad (14)$$

The Lucas-Washburn equation was found unable to predict liquid rise in the vertical PVOH coated FEP microcapillaries as shown in Fig. 3c, over-predicting the superficial flow velocity in the capillaries by up to one order of magnitude (Fig. 3d). For small values of H (therefore large values of 1/H) the superficial flow velocity in the individual capillaries was consistent with dH/dt values predicted for a pure discharge system represented by Equation 13.

It is unknown the reason why the direction of flow resistance or pressure head forces in Equation (12) is opposite that in Equation (2), but it appears that upon immersing the bottom tip of the PVOH coated microcapillaries in an aqueous liquid, the movement of the air-liquid meniscus is controlled by the speed of wetting, and the hydrophilic nature of the crosslinked PVOH coating creates a "pulling" force similar to that of a mechanical liquid pump. The liquid being "pulled" upwards in the hydrophilic capillary consequently behaves similarly to gravitational emptying of liquid from a vertical hydrophobic capillary. The contact angle appears relevant to set the direction for the force, yet the superficial flow velocity and flow resistance is not dependent on the surface tension forces during this stage of "continuous" liquid flow. This agrees with pressure balance models that governs e.g. continuous immiscible liquid-liquid flow in microcapillaries, see for example Scheiff et al.[34] Once H reached around 40% of the equilibrium Laplace height surface tension governs liquid rise in the capillary, with dH/dt following closely the analytical solution for the full pressure balance in Equation (11) (Fig. 3d).

Note that in order to accurately predict the Laplace height in the elliptical capillaries with Equation (11) – which is based on d_h, therefore only accurate for a circular capillary - a best-fitted value for surface tension was used instead, γ = 83.9 mN/m. This allowed reducing deviations of predicted maximum H from up to 24% down to up to 12%. The Lucas-Washburn equation was unable to predict a maximum liquid rise in a microcapillary, for not considering a maximum equilibrium height in the pressure balance equation.

The full pressure balance model herein presented is essential for understanding the dynamics of fluid wicking in the PVOH-coated microcapillaries, and future studies will look at integration of this model with the control of reagents release from the thin film in the microcapillaries.

Reagent loading

The reagents loading process proved effective for a wide range of assay reagents tested with a broad spectrum of physicochemical properties, ranging from small molecules such as sugars and organic dyes, through to large macromolecules such as antibodies (Table 2). We found that a very wide range of reagents could be loaded as a thin film in the MCF strips coated with crosslinked PVOH (as shown in Fig. 2b), followed by washing the strips with a small volume of water and performing appropriate analysis to the eluted samples to determine by mass balance the overall amount of reagents loaded and released. This is further detailed in Experimental Section in the manuscript. The mass fraction of reagents deposited and released varied from 0.8 wt% with Trimethoprim to 4.3 wt% with Glucose (Table 2). Viscosity and surface tension of each reagent solution was not measured, however there was a clear correlation between the increase in loading efficiency for more concentrated reagent solutions which is linked to a capillary number effect as detailed elsewhere.[35,36] The variable loading efficiency seen with some reagents in these proof-of-concept experiments (e.g. ciprofloxacin, Table 1) was subsequently found to be caused by

Table 2. Efficiency and thin film reagents deposition and release in Lab-on-a-Stick strips

Reagent[a]	Assay/Application	Loading solution concentration	Released concentration [a]	Loading efficiency wt%
Human IgG	Immunoassay	15.12 ± 0.02 mg/mL	0.41 ± 0.08 mg/mL	2.7
Mouse IgG	Immunoassay	900 ± 40 µg/mL	36 ± 9 µg/mL	3.9
Anti-A agglutinating reagent[b]	ABO blood typing	4.6 ± 0.4 mg/mL	0.098 ± 0.002 mg/mL	2.1
Anti-B agglutinating reagent	ABO blood typing	6.2 ± 0.09 mg/mL	0.18 ± 0.02 mg/mL	2.9
Anti-Rhesus agglutinating reagent	ABO blood typing	11 ± 0.1 mg/mL	0.28 ± 0.01 mg/mL	2.5
Glucose	Fermentation	500 mg/mL	21 ± 2 mg/mL	4.3
Trimethoprim	Antibiotic resistance	2.5 mg/mL	23 ± 11 µg/mL	0.8
Ciprofloxacin	Antibiotic resistance	3.0 mg/mL	51 ± 31 µg/mL	1.7

[a] Released concentrations represent mean ± 1 S.D of 3 replicate measurements. [b] ABO agglutinating reagents contained monoclonal agglutinating antibodies plus BSA carrier and therefore total protein concentration was measured.

manual reagent loading without carefully controlling the velocity of excess reagent removal, and can be reduced using constant airflow (e.g. using a syringe pump). Note that although loading/release efficiencies appear very low, residual reagent solution removed from the microcapillaries during the wall deposition procedure can be reused, reducing waste. We have subsequently developed a modified procedure that allows 100% efficiency for deposition of assay reagents in the PVOH coated microcapillaries, this will be subject of future publications.

The crosslinked PVOH coating was found to be unaffected by reagent loading or release steps. This hydrophilic coating was found to be very stable as ≥80mm capillary rise was observed in all 10 capillaries of >100 replicate test strips dipped into aqueous samples in many different locations after both extended storage at room temperature, and after international air transportation.

Other methods for entrapment and controlled release of reagents within glass channels and plastic capillaries have been developed in the past exploiting hydrogel layers attached to the internal surface of capillaries[37] and microchannels,[38] however these may be limited by the slow diffusivity of reagents through the porous hydrophilic layer, and may require reagent loading before assembly of microchannels. Our loading method is simpler, allows more rapid reagent release and efficient mixing with sample at the meniscus, and the use of MCF allows multiple parallel tests to be performed on a single sample. Confocal microscopy of fluorescent antibody confirmed a rapid radial mixing of reagent deposited on the thin film upon the rising of the meniscus, followed by a slower rate of reagent release from the thin film that appeared specific to the molecule (see Figs. S1 and S3). A possible drawback from this method highlighted from real time confocal fluorescence imaging was the development of a gradient of reagent concentration along the microcapillaries, with maximum concentration in the region around the meniscus. This is further detailed in ESI.

ABO blood typing

We demonstrated the suitability of the Lab-on-a-stick approach for performing assays on eukaryotic cells by developing improved ABO agglutination assays that allow multiplex testing with simplified detection of agglutination. We illustrated this concept by performing instantaneous ABO blood typing but the same principle is valid for related tests such as red blood cell or latex agglutination assays. Individual microcapillaries within a 2 m long hydrophilic coated MCF (Fig. 4a) were loaded with agglutinating antibodies against red blood cell antigens, in particular anti-A, anti-B and anti-D (rhesus factor), and the remaining 4 capillaries left unloaded (working as negative controls), and trimmed into 10 cm long dipsticks. Within few seconds of being dipped into reconstituted blood (with 40% red blood cell content), blood samples rose by capillary action up to ~80 mm in height. In microcapillaries loaded with agglutinating antibody against red

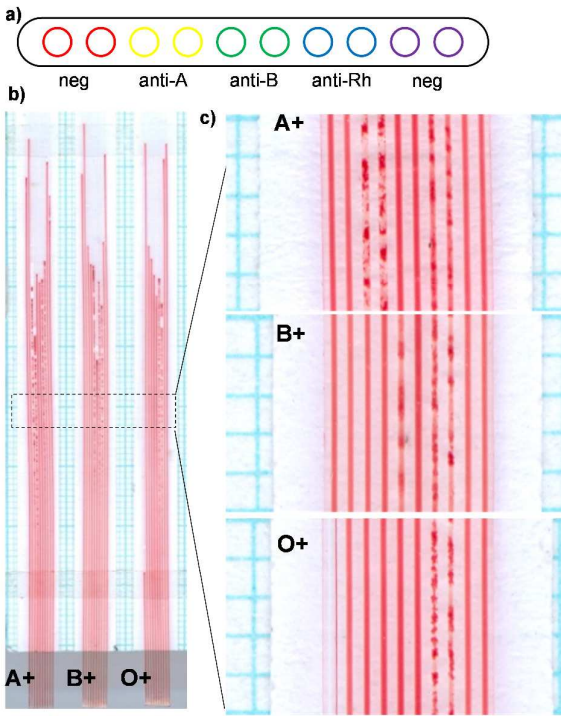

Fig. 4 Instantaneous ABO blood typing. a) Hydrophilic coated MCF test strips were loaded with A, B or rhesus blood antigen agglutinating antibodies. b) Test strips were dipped into blood samples and photographed after capillary rise was complete. c) Magnified images of ABO test strips showing capillaries with negative and positive agglutination; agglutination was observed only in capillaries where appropriate blood group antigens were present on RBCs. Image presented representative of >10 independent ABO agglutination assays in Lab-on-a-Stick test strips.

blood cell antigens, aggregation and clustering was rapidly observed indicating positive red blood cell agglutination (Fig. 4). In contrast, in control microcapillaries or those loaded with antibodies against RBC antigens not present on that sample, a uniform red colour was seen indicating lack of agglutination. This is further demonstrated in the film provided in ESI. Note that in enlarged images shown, capillary 6 for the B+ sample appears less obviously agglutinated than other agglutinated capillaries; in this particular capillary agglutination was more clearly apparent higher up the test strip.

The agglutination was most intense at the highest point of the blood filled microcapillary, and near the inlet no agglutination was detected, reflecting a more intense agglutination reaction near the meniscus of the fluid. This is linked to the rate of reagents release from the thin film and a level of convective release of reagents generated by the rising meniscus, as detailed in Figs. S1 and S3 in ESI. In addition, we noticed a reduced capillary rise in capillaries where agglutination was observed (Fig. 4b), this is clearer in strips loaded with only anti-A antibodies in Fig. S6b. A positive agglutination reaction results in strong binding of RBCs that leads to changes in viscosity and surface tension of the solution, consequently changes in equilibrium liquid height. We also noticed distinct rates of reaction of the different agglutination antibodies, consequently the variability in the terminal liquid height in the multiplexed tests shown in Fig. 4 is intrinsically linked to the combined effect of the rate of release of reagents, the rate of agglutination reaction and changes in physical properties of the fluid.

Potentially the loading and release of reagents from the thin film in the Lab-on-a-Stick can be optimised for enhancing positive/negative discrimination of the agglutination reaction. In addition, agglutination in microcapillaries provide very clear and simple optical detection of agglutination that is not possible in conventional Eldon card or on a transparent glass slide, as shown in Fig. S6 in ESI.

Bacterial identification testing

The Lab-on-a-Stick is also ideally suited to performing assays on prokaryotic cells. We successfully multiplexed and miniaturised classical analytical microbiology tests for phenotypical identification of bacteria and for quantitative measurement of antibiotic susceptibility. These two critical and routine microbiology tests are still confined to the laboratory, and cost-effective rapid and portable versions of laboratory microbiology tests are urgently needed.[39] To perform phenotypical identification tests, a panel of sugars was loaded within individual microcapillaries in an hydrophilic coated fluoropolymer MCF at sufficient concentrations to perform fermentation assays in the microcapillaries (Fig. 5a). When test strips were dipped into bacterial colonies resuspended in fermentation medium containing the classical pH indicator phenol red, only in the presence of bacteria capable of fermenting each particular sugar did the pH indicator change colour indicating media acidification (Fig. 5b). This allowed discrimination between *E. coli* and Salmonella based on lactose fermentation; *E. coli* and *Salmonella enterica*

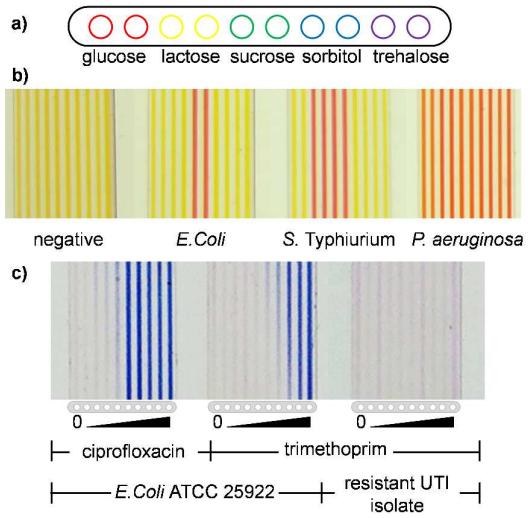

Fig. 5 Microfluidic dipstick bacterial identification and antibiotic susceptibility testing. a) Hydrophilic coated FEP MCF was bulk loaded with the 5 indicated sugars, and test strips cut and dipped into individual colonies of the indicated bacteria resuspended in an orange pH indicator broth. b) After 4 h incubation, bacteria capable of fermenting each sugar produced a yellow colour indicating acidification, in contrast to orange-red colour indicating no fermentation. c) MIC test strips loaded with serial dilutions of the indicated antibiotics were dipped into *E. coli* samples resuspended in resazurin indicator medium, and imaged after overnight incubation. Bacterial growth converted the blue medium through pink to white, and capillaries remained blue when antibiotic concentration sufficient to inhibit growth. Example images of fermentation assays are representative of multiple assays performed with more than 5 different sugars and multiple bacterial samples, and MIC assays are representative of multiple MIC assays performed with a total of 4 different antibiotics and 3 different bacterial strains. Note that image contrast and brightness was adjusted equally for all test strip images.

are phenotypically very similar, but only *E. coli* ferments lactose. In contrast, when unable to ferment the sugar, metabolism of media components raised the pH leading to a change from orange to pink. Likewise, with the non-fermenting control organism *P. aeruginosa*, pH was raised in the presence of all sugars, giving pink colour. Thus careful selection of an intermediate orange indicator colour for the indicator medium allowed for detection of both fermentation lowering pH, and metabolism of other energy sources raising pH.

Although fermentation assays are not alone able to definitively identify bacterial species, they remain the single most commonly used and internationally accepted microbial identification assays. The more different fermentation substrates tested, the more reliably a bacterial sample can be identified, therefore this exemplar cellular assay demonstrates clearly the advantage of low cost multiplex MCF test strips where 10 tests can be performed per test strip, and multiple strips can be used to test a single sample to increase multiplexing beyond 10 assays. The second most common test is enzymatic assays e.g. using colorimetric substrates such as ONPG for beta-galactosidase enzyme, which are likewise ideally suited to performing in Lab-on-a-Stick test strips. As an example, we demonstrated that the antibiotic resistance enzyme beta-lactamase could be rapidly detected in MCF using the chromogen nitrocefin (Fig S4).

Functional minimum inhibitory concentration assays

Given the rise of antimicrobial resistance, it is critically important that we develop improved antibiotic resistance tests. We developed a dipstick microfluidic minimum inhibitory concentration (MIC) assay to quantify antibiotic susceptibility which detects the lowest concentration of antibiotic that inhibits growth. Individual microcapillaries in were loaded with 2-fold serial dilutions of antibiotics, and 30 mm Lab-on-a-Stick MIC test strips were dipped into *E. coli* samples resuspended in resazurin growth indicator medium. Following incubation, when bacteria grew inside microcapillaries the indicator medium changed from blue to pink indicative of conversion of resazurin to resorufin, and eventually to white at high bacterial cell density after overnight incubation. In the MIC test strips, colour changed from blue to white only in microcapillaries where the antibiotic concentration was too low to inhibit cell growth. At higher concentrations of antibiotic the capillaries remained blue, demonstrating growth inhibition and thereby the minimal inhibitory concentration (Fig. 5c).

Note that although FEP is relatively oxygen permeable as previously reported,[40] we have not yet determined the accessible oxygen levels within MCF test strips, as in common with many other clinically and industrially important bacteria, *E. coli* are facultative anaerobes and grow both in the presence and absence of oxygen.

MIC values in microfluidic dipstrips were measured by calculating the released concentration of antibiotic in the last capillary that remained blue by multiplying the loading solution concentration by the antibiotic loading efficiency in Table 2. Similar MIC values were obtained to those measured using a conventional resazurin microplate (Fig. S7 and Table S1) method with ATCC 25922 *E. coli* strain showing MIC of 0.24 µg/mL, and 0.011 µg/mL for trimethoprim and ciprofloxacin respectively when measured in Lab-on-a-Stick dipstrips, compared to 0.25 µg/mL and 0.015 µg/mL measured in microplates (Fig. 5c). When clinical *E. coli* urinary tract infection (UTI) isolates were tested, for many samples cell growth was observed in all capillaries indicating antibiotic resistance. Antibiotic resistance observed in Lab-on-a-Stick MIC tests on clinical UTI isolates matched the resistance profile determined using conventional disc diffusion methods. Note that a gradient of cell growth is visible in capillaries at threshold concentrations of antibiotics. This reflects the gradient of antibiotic released into the sample as it rises into the microcapillary, with the highest concentration at the top showing stronger blue colour in contrast to the lower concentration at the bottom where growth is detectable. This gradient of reagent concentration is further detailed in Fig. S2 and found to be minimised by having shorter test strips, potentially providing additional quantitative information about antibiotic susceptibility.

It is important to understand that small variations in bacterial growth and cell density in the presence of a marginal concentration of antibiotic lead to variable MIC observed. This is true even with internationally recognised standardised microplate MIC assays, and with internationally accepted standard reference strains of *E. coli*, variations over a 4-fold range are considered acceptable.[41] Indeed, the parallel microplate assays performed alongside Lab-on-a-Stick tests showed 2 to 4-fold variation in observed MIC between two repeat tests (see Fig. S4 in ESI). What is critical is to measure order of magnitude changes in antibiotic sensitivity, with MIC typically tested over a 100-1000-fold range.

The antibiotic loading solution in these proof-of-concept studies were manually removed using a syringe to drive air through, which led to relatively high variation in antibiotic loading seen in Table 1. However, this variation can be eliminated by loading using syringe pumps, and the inherent variation in MIC measurements over a 2- to 4-fold range means that the manually prepared strips remained highly informative in spite of this variability in antibiotic loading.

Conclusions

The new Lab-on-a-Stick approach is simple yet flexible, uniquely combining the benefits of conventional dipstick tests with the capabilities of microfluidic systems. The coating of FEP microcapillaries with crosslinked PVOH allows in one step both reduces the contact angle of the FEP microcapillaries for sample uptake by capillary action, and facilitates *in situ* assay reagent delivery. Sample uptake by capillary action is predictable with a full pressure balance, which considers surface tension, resistive and pressure head forces. Lab-on-a-stick provides a cost-effective, simple, portable and flexible multiplex platform for a range of assays, and this proof-of-concept study should lead to the development of a new generation of advanced yet affordable point-of-care tests for global applications.

Acknowledgements

Authors are grateful to Patrick Hester for providing the MCF material, and to EPSRC (grant EP/L013983/1) and Loughborough University for funding.

References

1 C. D. Chin, V. Linder and S. K. Sia, *Lab Chip*, 2012, **12**, 2118–34.
2 M. Focke, D. Kosse, C. Müller, H. Reinecke, R. Zengerle and F. von Stetten, *Lab Chip*, 2010, **10**, 1365–86.
3 W. Zhao and A. van der Berg, *Lab Chip*, 2008, **8**, 1988–1991.
4 A. W. Martinez, S. T. Phillips, M. J. Butte and G. M. Whitesides, *Angew. Chem. Int. Ed. Engl.*, 2007, **46**, 1318–20.
5 A. W. Martinez, S. T. Phillips, G. M. Whitesides and E. Carrilho, *Anal. Chem.*, 2010, **82**, 3–10.
6 G. G. Lewis, M. J. Ditucci and S. T. Phillips, *Angew. Chemie - Int. Ed.*, 2012, **51**, 12707–12710.
7 B. S. Lee, J.-N. Lee, J.-M. Park, J.-G. Lee, S. Kim, Y.-K. Cho and C. Ko, *Lab Chip*, 2009, **9**, 1548–1555.
8 H. Ramachandraiah, M. Amasia, J. Cole, P. Sheard, S. Pickhaver, C. Walker, V. Wirta, P. Lexow, R. Lione and A. Russom, *Lab Chip*, 2013, **13**, 1578–85.
9 M. . Mancuso, L. . Jiang, E. . Cesarman and D. . Erickson, in *Proceedings of the 16th International Conference on*

Miniaturized Systems for Chemistry and Life Sciences, MicroTAS 2012, Chemical and Biological Microsystems Society, Okinawa, 2012, pp. 1360–1362.
10 A. Grimes, D. N. Breslauer, M. Long, J. Pegan, L. P. Lee and M. Khine, *Lab Chip*, 2008, **8**, 170–172.
11 B. Ngom, Y. Guo, X. Wang and D. Bi, *Anal. Bioanal. Chem.*, 2010, **397**, 1113–1135.
12 G. a Posthuma-Trumpie, J. Korf and A. van Amerongen, *Anal. Bioanal. Chem.*, 2009, **393**, 569–82.
13 C. D. Chin, T. Laksanasopin, Y. K. Cheung, D. Steinmiller, V. Linder, H. Parsa, J. Wang, H. Moore, R. Rouse, G. Umviligihozo, E. Karita, L. Mwambarangwe, S. L. Braunstein, J. van de Wijgert, R. Sahabo, J. E. Justman, W. El-Sadr and S. K. Sia, *Nat. Med.*, 2011, **17**, 1015–9.
14 T. Kawabata, H. G. Wada, M. Watanabe and S. Satomura, *Electrophoresis*, 2008, **29**, 1399–1406.
15 L. Gervais and E. Delamarche, *Lab Chip*, 2009, **9**, 3330–7.
16 D. Juncker, H. Schmid, U. Drechsler, H. Wolf, M. Wolf, B. Michel, N. De Rooij and E. Delamarche, *Anal. Chem.*, 2002, **74**, 6139–6144.
17 G. M. Walker and D. J. Beebe, *Lab Chip*, 2002, **2**, 131–134.
18 M. L. Sin, J. Gao, J. C. Liao and P. K. Wong, *J. Biol. Eng.*, 2011, **5**, 6.
19 D. Desai, G. Wu and M. H. Zaman, *Lab Chip*, 2011, **11**, 194–211.
20 C. Rivet, H. Lee, A. Hirsch, S. Hamilton and H. Lu, *Chem. Eng. Sci.*, 2011, **66**, 1490–1507.
21 H. Wakayama, T. G. Henares, K. Jigawa, S. Funano, K. Sueyoshi, T. Endo and H. Hisamoto, *Lab Chip*, 2013, **13**, 4304–4307.
22 Y. Fujii, T. G. Henares, K. Kawamura, T. Endo and H. Hisamoto, *Lab Chip*, 2012, **12**, 1522–1526.
23 Y. Uchiyama, F. Okubo, K. Akai, Y. Fujii, T. G. Henares, K. Kawamura and T. Yao, *Lab Chip*, 2012, **12**, 204–208.
24 A. P. Castanheira, A. I. Barbosa, A. D. Edwards and N. M. Reis, *Analyst*, 2015, **140**, 5609–18.
25 A. I. Barbosa, A. P. Castanheira, A. D. Edwards and N. M. Reis, *Lab Chip*, 2014, 2918–2928.
26 A. I. Barbosa, P. Gehlot, K. Sidapra, A. D. Edwards and N. M. Reis, *Biosens. Bioelectron.*, 2015, **70**, 5–14.
27 G. V. Kaigala, R. D. Lovchik and E. Delamarche, *Angew. Chemie - Int. Ed.*, 2012, **51**, 11224–11240.
28 G. M. Whitesides, *Nature*, 2006, **442**, 368–373.
29 B. Hallmark, F. Gadala-Maria and M. R. Mackley, *J. Nonnewton. Fluid Mech.*, 2005, **128**, 83–98.
30 A. D. Edwards, N. M. Reis, N. K. H. Slater and M. R. Mackley, *Lab Chip*, 2011, **11**, 4267–4273.
31 G. E. McCreath, R. O. Owen, D. C. Nash and H. a Chase, *J. Chromatogr. A*, 1997, **773**, 73–83.
32 M. Kozlov, M. Quarmyne, W. Chen and T. J. McCarthy, *Macromolecules*, 2003, **36**, 6054–6059.
33 B. Lutz, T. Liang, E. Fu, S. Ramachandran, P. Kauffman and P. Yager, *Lab Chip*, 2013, **13**, 2840–7.
34 F. Scheiff, M. Mendorf, D. Agar, N. Reis and M. Mackley, *Lab Chip*, 2011, **11**, 1022–1029.
35 C. Eaboratory and B. G. I. Taylor, *J. Fluid Mech.*, 1961, **10**, 161–165.
36 B. F. P. Bretherton, *J. Fluid Mech.*, 1960, **10**, 166–188.
37 M. Kataoka, H. Yokoyama, T. G. Henares, K. Kawamura, T. Yao and H. Hisamoto, *Lab Chip*, 2010, **10**, 3341–3347.
38 M. Beck, S. Brockhuis, N. van der Velde, C. Breukers, J. Greve and L. W. M. M. Terstappen, *Lab Chip*, 2012, **12**, 167–73.
39 S. Cohen-Bacrie, L. Ninove, A. Nougairède, R. Charrel, H. Richet, P. Minodier, S. Badiaga, G. Noël, B. la Scola, X. de Lamballerie, M. Drancourt and D. Raoult, *PLoS One*, 2011, **6**.
40 K. S. Elvira, R. C. R. Wootton, N. M. Reis, M. R. Mackley and A. J. deMello, *ACS Sustain. Chem. Eng.*, 2013, **1**, 209–213.
41 J. M. Andrews, *J. Antimicrob. Chemother.*, 2001, **48 Suppl 1**, 5–16.

SUPPLEMENTARY DATA

Lab on a Stick: Multi-Analyte Cellular Assays in a Microfluidic Dipstick

Nuno M. Reis,[a] Jeremy Pivetal,[b] Ana L. Loo-Zazueta,[a] João M.S. Barros,[b] and Alexander D. Edwards*[b]*

[a]Department of Chemical Engineering, Loughborough University, Leicestershire, LE11 3TU, UK. Fax: +44(0) 1509 223 923; Tel. +44(0) 1509 222 505; E-mail: n.m.reis@lboro.ac.uk

[b]Reading School of Pharmacy, University of Reading, Whiteknights, Reading RG6 6AD, UK. Fax: +44 (0) 118 378 6562; Tel: +44(0) 118 378 4253; E-mail: a.d.edwards@reading.ac.uk

Supplementary Methods

Scanning Electron Microscopy (SEM)

A Carl Zeiss (Leo / Cambridge) 360 SEM was used for scanning the characteristics of inner surfaces of the PVOH-coated microcapillaries. A scanning electron microscope works by focusing a beam of high energy electrons to produce a variety of signals at the surface of the sample, and the signals generated from the electron-sample interactions provide information about the sample including morphology, chemical composition, and crystalline structure. MCF samples were prepared by gently drying the capillaries with nitrogen and slicing the strips along and through the middle of the capillaries in order to reveal the inner surface of the microcapillaries. The length of the samples scanned were about 4 mm, which was fixed to a pin stub mount with double-side tape. Samples where coated with a thin 20nm layer of gold using an Edwards S150 bench-top sputter coater for 60 seconds.

Atomic Force Microscopy (AFM)

AFM is a powerful technique for imaging surfaces at micrometre or nanometre resolution. In contrast to SEM, it does not require samples to be conductive or metal-coated. A Veeco atomic

force microscope (Model Explorer) with both non-contact and pulsed force imaging modes was used to obtain topography images of the uncoated and coated MCF microcapillaries. Strips were cut along the capillaries at an angle (starting from the middle part of the microcapillary) to allow the AFM probe to reach the inner surface of the microcapillaries.

Confocal fluorescence imaging of reagents release

Dried PVOH-coated strips were loaded with 1 mg/mL of mouse anti-human IgM or IgG fluorescently labelled with FITC (Sigma-Aldrich, Dorset, UK) and incubated for at least 2 hours, after which the excess of reagent was removed by flushing the capillaries with air. The MCF strips were then examined using a Nikon TE300 inverted microscope equipped with a Bio-Rad Radiance 2000 confocal laser scanning head. A Nikon 10x/0.25 Ph1 DL objective lens was used for imaging. The confocal microscope was computer controlled using the software LaserSharp 2000 (Bio-Rad), equipped with argon laser with peak excitation 488 nm and long pass 500 nm filter. The laser intensity, scan speed (500 lines per secod), iris, gain, offset and resolution (512 pixels * 512 pixels) were all kept constant, meaning results from multiple replicas and runs are directly comparable quantitatively.

Microtiter plate MIC assays

Samples of *E. coli* from a reference strain (ATCC) and *E. coli* clinical isolate from a UTI patient that were tested with MCF Lab-on-a-Stick test strips (Fig. 5c) were also tested in parallel following the standardized protocol fully described in literature.[1]

Supplementary Results

Analysis of concentration gradient along the microcapillaries

Detailed confocal fluorescence imaging of *in-situ* release of IgM and IgG in the PVOH-coated strips revealed a gradient of concentration along the strip which varies with the length of the strip but also with the reagent type. The strips where scanned along the entire length once the meniscus reached the equilibrium height. In the case of Fig. S1 the release of IgM and IgG was directly compared and showed a sharper concentration gradient for the smaller molecule (i.e. IgG).

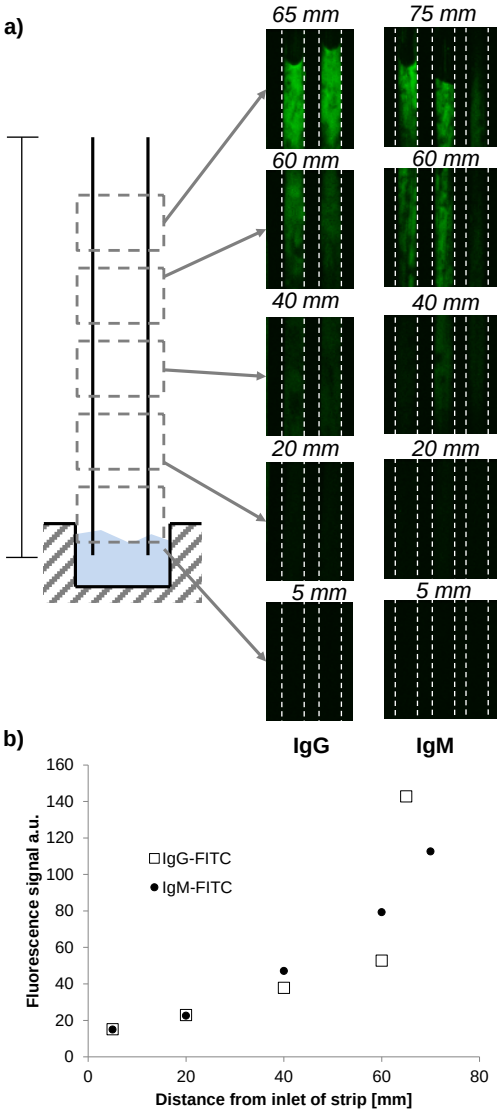

Fig. S1 Confocal imaging of reagents release in PVOH-coated microcapillaries. All capillaries in the same strip were loaded with same reagent (IgM-FITC or IgG-FITC at 1 mg/ml), and the strips imaged once the meniscus reached the equilibrium height. Images show the capillaries in the centre of the strip at middle height of the capillary, at the axial distance shown in the labelling.

A similar study examined the concentration gradient when colored reagents were loaded and released from hydrophilic-coated MCF test strips. As an example, we selected an important colorimetric enzyme for detecting antibiotic resistance. Beta-lactamase enzymes can degrade antibiotics of the beta-lactam class (e.g. penicillins, crbapenems) and these resistance enzymes are a major global threat. Some beta-lactamase enzymes can be rapidly detected using yellow colorimetric substrate nitrocefin, which is turned red in the presence of beta-lactamase enzymes. Hydrophilic coated MCF was loaded with 10mg/mL nitrocefin dissolved in DMF, and the loading solution gently removed with air using a syringe. As expected, when long (6cm) test strips were dipped into water, a yellow colour was seen (Fig. S2) whereas when dipped into a beta-lactamase enzyme solution, a strong red colour was observed indicating rapid enzymatic conversion of nitrocefin. The reagent gradient was clearly visible, with the top (i.e. near meniscus) showing most intense colour indicating highest reagent concentration, as seen with antibody reagent in Fig S1. This gradient could be quantified by plotting an intensity plot for the blue channel (Fig. S2b). In contrast, a uniform colour was observed when 1mg/mL solutions of nitrocefin or enzymatically converted red product were loaded into MCF strips (Fig. S2c). In spite of the gradient of reagent release, the colour change was evident along the length of the strip, and as evident from the profile plots the dye reagent could be quantified at both the inlet and the meniscus.

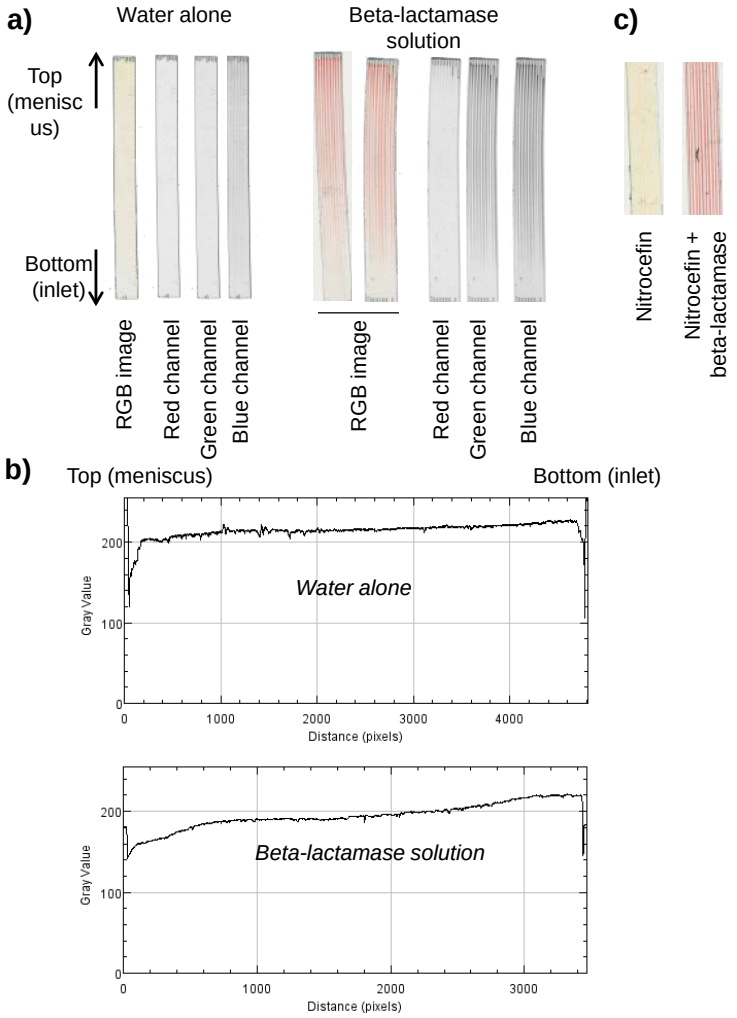

Fig. S2 Demonstration of gradient of antibiotic resistance enzyme reagent released from Lab-on-a-Stick test strips. a) hydrophilic coated MCF was loaded with 10 mg/mL nitrocefin in DMF, loading solution removed using air, and short test strips cut. These were dipped either into water alone or a solution of beta-lactamase enzyme. Images illustrate RGB image, and greyscale images of the three colour channels split to see the increase in green absorbance on enzymatic conversion, leading to the colour change from yellow to red. b) The blue channel intensity was plotted along the length of a single capillary to illustrate the variation in reagent concentration from the top (meniscus) to the bottom (inlet) of the test strip. c) Solutions of 1mg/mL nitrocefin with or without beta-lactamase enzyme were prepared in microtubes, then filled into MCF strips to illustrate the uniform colour when reagent was directly filled into microcapillaries.

Analysis of reagents release from the thin film

A further set of confocal imaging experiments aimed studying the dynamic release of reagents from the thin film as shown in Fig. S3 and further understand the concentration gradients observed e.g. in Fig. 4, Fig. 5 or Fig. S2. All capillaries were loaded with 1 mg/ml of mouse anti-human IgG or IgM fluorescently labelled with fluorescence FITC similar to data in Fig. S1. Capillaries where observed to flow at different time points, this is linked to some variability in the contact angle in the capillaries in this particular experimental setup, which required taping a section of the strip on a glass slide for imaging in the microscope and carefully adding a small volume of PBS buffer in the area around the inlet of the strip.

Fig. S3 shows confocal images of a set of microcapillaries during capillary rise of PBS buffer in strips pre-loaded with IgM-FITC or IgM-FITC. Initially, only a thin layer of FITC labelled antibody is visible in the image on the internal wall of the microcapillary at time 0; note the *z* height of the stack selected was halfway through the height of the microcapillary, therefore two side walls are visible in the image in Fig. S3a. During capillary rise of liquid in the capillaries (it took few seconds for liquid to be detected in the first capillary) it is well visible the higher concentration of reagent dragged by the meniscus, which is further highlighted in Fig. S3b. Once liquid has reached equilibrium height in the capillary, the FITC labelled antibody could be detected everywhere across the capillary (Figure S3c), especially near the walls and quickly diffused towards the centre of the capillary. It was noticed a major difference in diffusion rates of IgM and IgG molecules from the thin film as shown in Fig. S3d, which is linked to very distinct molecular weight of these two antibody molecules. It is believed the concentration gradient generated along the microcapillaries result from the combined effect of the meniscus and passive diffusion of molecules from the thin film, and can be controlled by manipulating diffusion rate of reagents and/or the length of the microcapillary strip.

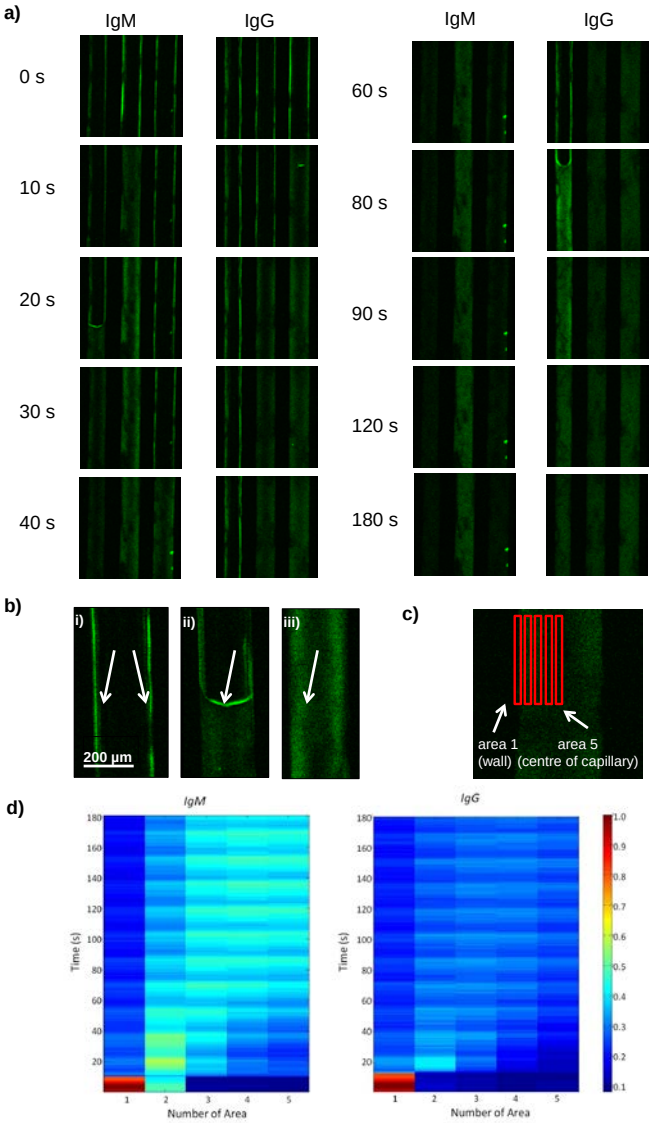

Fig. S3 Kinetic analysis of reagents release in FEP microcapillaries coated with crosslinked PVOH with confocal microscopy. a) Release of IgM-FITC or IgG-FITC imaged at 60 mm from the inlet of the strip (stacks show 3 capillaries in the centre of the strip at middle height in the capillaries). b) Key features of *in-situ* reagents release, showing in (i) a thin film of FITC-IgG deposited onto the hydrophilic capillary - the arrows point to the position of the walls, (ii) PBS buffer rising into capillary – the arrow points to the position of the rising meniscus and in (iii) release of FITC-IgG by diffusion– the arrow points to the area with the highest antibody concentration. c) Areas of the capillaries where fluorescence signal was interrogated with time allowing to study reagents release from the thin film and diffusion across the microcapillaries. d) Normalised mean fluorescence intensity for the capillaries in the centre of the images in a) for the areas of identified in c).

Surface characterization of the inner surface of POVH-coated microcapillaries

SEM and AFM analysis (Figs. S4 and S5, respectively) to the inner surfaces of the microcapillaries revealed the PVOH-coating is homogeneous along and across the microcapillaries. In particular, AFM images show the surface topography of PVOH-coated capillaries is very distinct from that of uncoated microcapillaries.

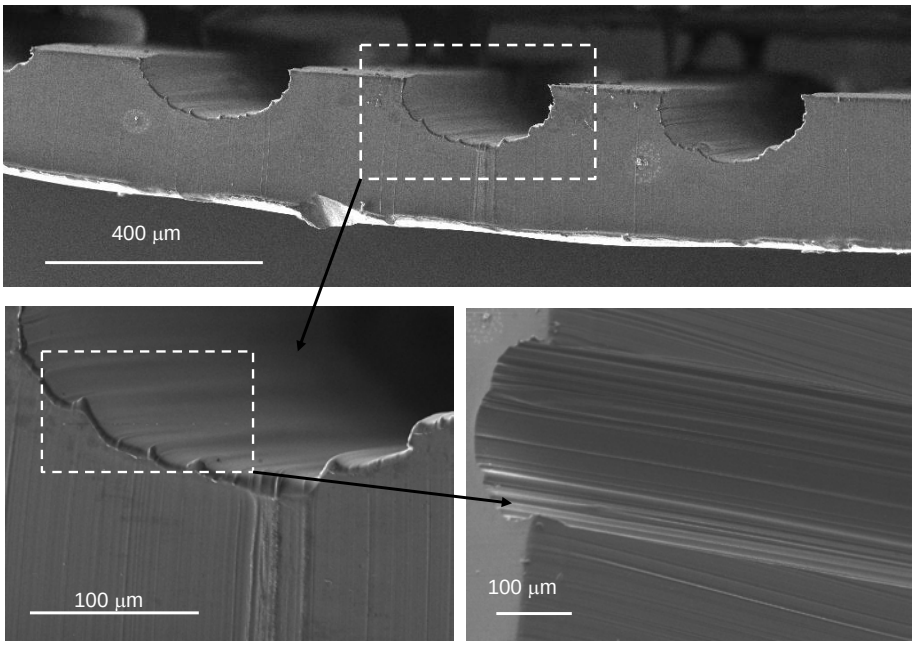

Fig. S4 Scanning Electron Microscopy image of MCF coated with PVOH, showing a smooth and evenly coated surface. The ridges along the capillaries are due to the cooling during the melt-extrusion process, being also observed in uncoated MCF material (image not shown).

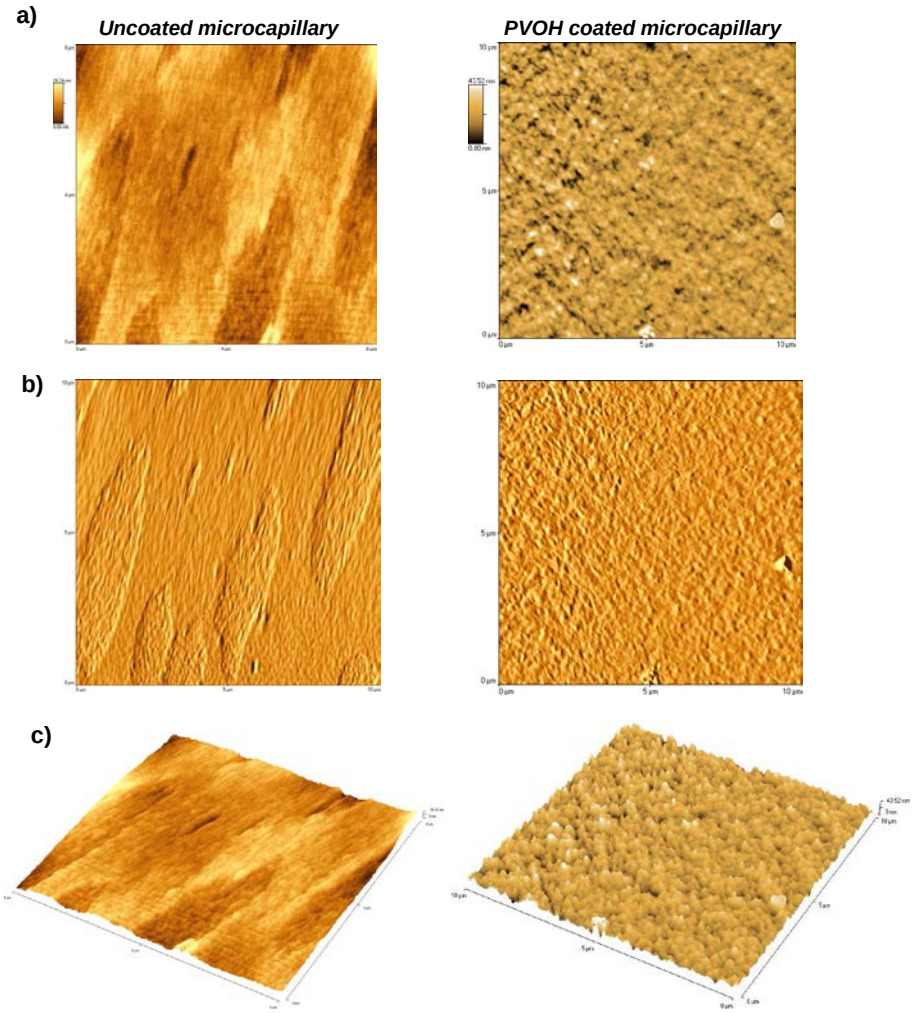

Fig. S5 AFM images of 10 μm x 10 μm areas in the inner walls of uncoated and PVOH-coated microcapillaries in Tapping (i.e. contactless) Mode. a) 2D topography (true height). B) Error or Tip Deflection. C) 3D Topography.

Clear optical detection of red blood cells agglutination in the microcapillaries

The profile plots for positive and negative agglutination were remarkably distinct when agglutination happens within the capillaries (Fig. S6b), being very difficult so differentiate positive agglutination from sample drying when the test is performed on a flat surface like a glass slide or even Eldon card as shown in Fig. S6a. Note the very consistent capillary rise within the same strip, and the reduced capillary rise in the agglutinated sample (Fig. S6b), which explains the variability in capillary rise in the multiplexed blood agglutination strips in Fig. 4.

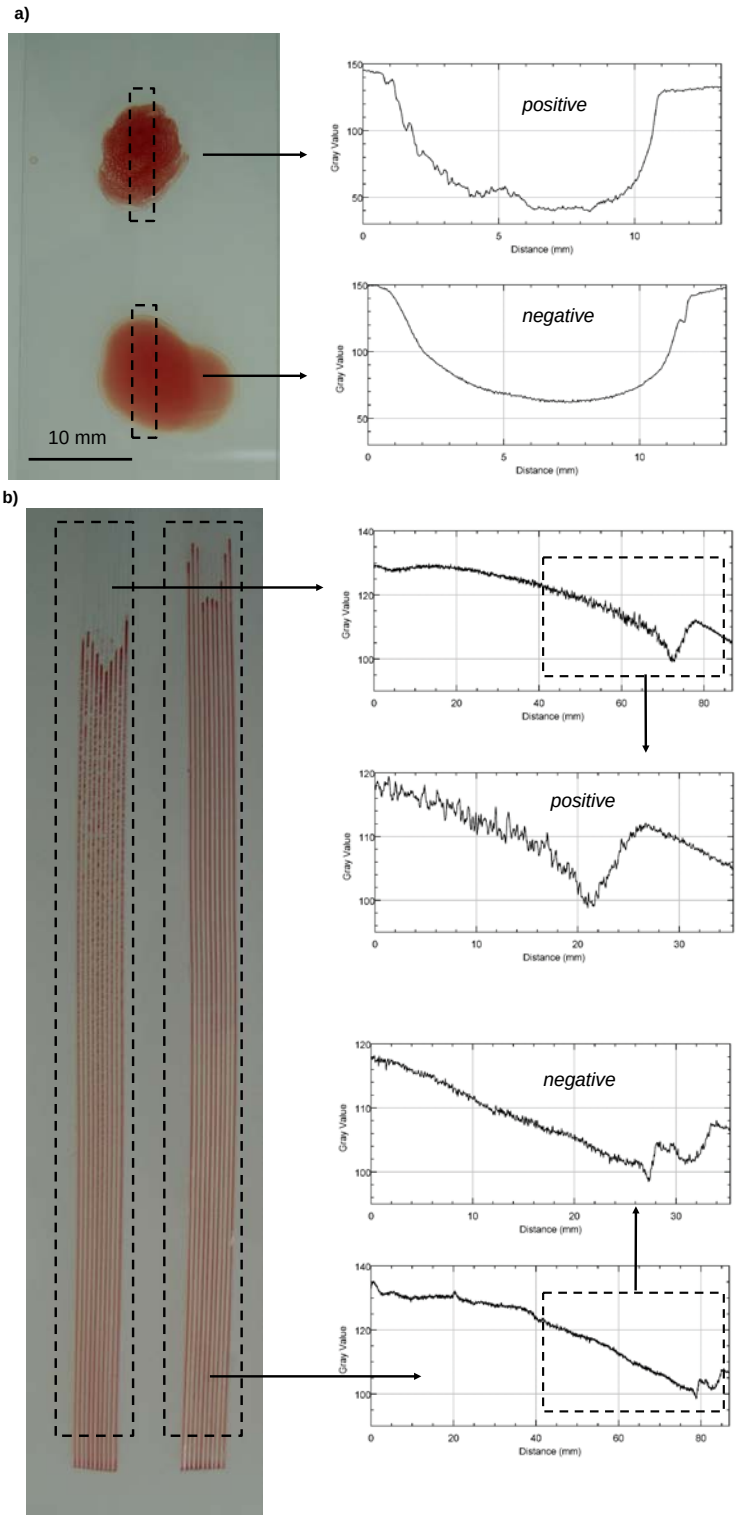

Fig. S6 Greyscale profile plots obtained with agglutinated and non-agglutinated blood samples. a) Testing on a transparent glass slide, where anti-A antibody was mixed with blood sample using pipette tip. b) Testing in the PVOH-coated MCF; all 10 capillaries where pre-loaded with anti-A reagent which was released and mixed with the sample during rising of blood sample by capillary action.

MIC assays in microtiter plates

To compare the performance of antibiotic loaded MCF Lab-on-a-Stick test strips for MIC assays with current 'gold standard' microtiter plate MIC assays, the same samples of *E. coli* reference strain (ATCC) and *E. coli* clinical isolate from a UTI patient were tested in parallel using the standardized protocol available in literature,[1] and also compared to the range of MIC values for the reference strain also published in Andrews[1] (Fig. S4 and Table S1). The MIC observed in the microplate correlated well with both the published reference values and with the values observed in the MCF test strips. However, it is important to note the even this standard reference protocol is inherently variable, and the published standard method indicates that even for reference strains significant assay-to-assay variation is expected:[1]

"*The MIC for the control strain should be within plus or minus one two-fold dilution of the expected MIC*"

In other words, there is an expectation of variation either one well higher or one well lower concentration than the published reference concentration. Indeed even with this 'gold standard' internationally agreed reference microplate method we do observe variation between replicate microplate tests, with the reference strain having 2-fold lower MIC in 2nd replicate than 1st replicate, and 4-fold lower MIC observed in 2nd replicate than first replicate (Fig. S7). Similarly, although resistant to 3 tested antibiotics, the UTI isolate shows 2-fold lower MIC in 2nd replicate than 1st replicate.

Table S1. Antibiotic concentrations used in microtitre plate MIC assays shown in Fig. S7, and comparison with threshold values and expected MIC values taken from Andrews[1]

		Gentamicin	*Tetracycline*	*Trimethoprim*	*Ciprofloxacin*
	E. Coli 25922 reference MIC (mg/L)[a]	0.5	2	0.25	0.015
	Resistant:	≥ 2	≥ 2	≥ 4	≥ 2
	Sensitive:	≤ 1	≤ 1	≤ 0.05	≤ 1
Concentration (mg/L)	Row 1	1	8	2	0.5
	Row 2	0.5	4	1	0.25
	Row 3	0.25	2	0.5	0.125
	Row 4	0.125	1	0.25	0.063
	Row 5	0.063	0.5	0.125	0.031
	Row 6	0.031	0.25	0.063	0.016
	Row 7 (no ABX)	0	0	0	0
	Row 8 (no cell control)	No cells	No cells	No cells	No cells

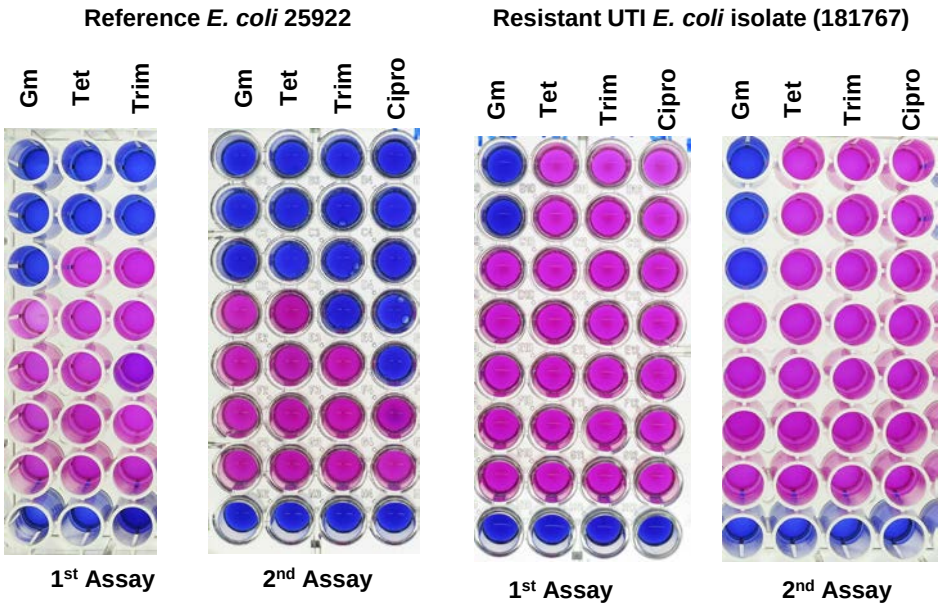

Fig. S7 Example of conventional microtitre plate MIC assay results.

Supplementary references

1 J. M. Andrews, *J. Antimicrob. Chemother.*, 2001, **48 Suppl 1**, 5–16.